

Bona fide stochastic resonance and multimodality in the stochastic Hodgkin-Huxley neuron

Sang-Gui Lee and Seunghwan Kim

AsiaPacific Center for Theoretical Physics, National Core Research Center on System BioDynamics, and Nonlinear and Complex Systems Laboratory, Department of Physics, Pohang University of Science and Technology, San 31 Hyojadong, Pohang, Korea 790-784

(Received 3 November 2003; revised manuscript received 4 March 2005; published 12 December 2005)

The phenomena of stochastic resonance (SR) has attracted much attention in the studies of the excitable systems, in particular, the nervous systems under noise. Recently, an alternative SR condition, called the bona fide SR, was proposed for the bistable system under noise, based on the notion of the residence time distribution. As the forcing frequency increases, there exists an optimal resonant frequency. We study the SR in a stochastic Hodgkin-Huxley neuron, which has an inherent natural frequency in addition to the stochastic time scale. We have observed two resonant conditions; one between periodic forcing and natural frequencies, and the other between the periodic forcing and the stochastic frequencies. These resonance conditions show the bona fide stochastic resonance with multimodality. For comparison, we have studied the bona fide SR in the stochastic FitzHugh-Nagumo neuron, where, the multimodality is not observed. The differences in the resonance structure of two neuron models are understood in terms of differences in the phase portraits.

DOI: [10.1103/PhysRevE.72.061906](https://doi.org/10.1103/PhysRevE.72.061906)

PACS number(s): 87.19.La, 05.40.Ca

In the last decades, the phenomena of the stochastic resonance (SR) [1] has attracted much attention [2–4] in the studies of noisy systems. SR is a phenomenon in which the responses of a nonlinear system to a weak periodic signal are optimized by suitable noise. In neural systems, the SR means that a neuron can utilize the environmental noise to detect a weak signal efficiently and enhance the signal transduction through it. A number of experiments on various neural systems have been reported to exhibit such nonlinear phenomena and much theoretical works have attempted to explain this sensing mechanism through studies of various neural systems [5–7].

An alternative SR condition is recently proposed in the bistable system through the analysis of the residence time distribution function [8]. They have observed the SR as a function of the modulation frequency, which is called as the *bona fide* stochastic resonance. This resonance is between the forcing frequency and the stochastic time scale. In comparison with the bistable system, the excitable systems including neuronal systems possess another important time scale corresponding to the inherent natural frequency. Thus, the stochastic neuron under periodic forcing has attracted much attention because the nonlinear coupling between these three frequencies may lead to the different resonance phenomena from those found in the bistable system [9,10]. For example, the parameter dependence of SR in the stochastic neuron may show a bell-shaped structure with a minimum near the inherent natural frequency, which has not been observed in the bistable system [10].

Even though the importance of bona fide stochastic resonance in the stochastic excitable system has been discussed in numerous works [9], the bona fide stochastic resonance in the excitable system has not been studied systematically through the measure of the strength of peaks in the interspike interval distribution function (ISIH) as a function of the forcing frequency. In this paper, we study the bona fide stochastic resonance in a stochastic Hodgkin-Huxley (HH) neuron focusing on the interactions between three frequencies in the resonance phenomena. We have found interesting phenom-

ena of multimodality in the bona fide stochastic resonance, which is caused by two different types of resonance conditions; a noise-independent one between periodic forcing and natural frequencies and the other noise-dependent one between periodic forcing and stochastic frequencies. In the study of the coherence resonance, the stochastic HH neuron and the stochastic FitzHugh-Nagumo neuron show very different resonance structures under dc current [11,12], in particular, due to the rigidity of the firings in the HH neuron. Likewise, we have studied the difference between the bona fide SRs in the FitzHugh-Nagumo and HH neurons. We have found that they show different resonance structures, which can be understood through the phase portrait analysis of two neurons.

The HH neuron, which is derived from the biophysical analysis of the squid giant axon [13], shows typical dynamics of a real neuron, the spiking behavior and the refractory period, and serves as a canonical model for tonically spiking neurons based on nonlinear conductances of ion channels. This HH neuron consists of four nonlinear coupled ordinary differential equations, one for the membrane potential V and the other three variables m, n, h for ion-channel gatings [13]. The large change of m, n, h variables, which are connected to the opening and closing of relevant ion channels, causes the neuron to show the rapid change in the membrane potentials, which is called as the action potential, or the spike. The membrane potential V is given by

$$\frac{dV}{dt} = I_{\text{ion}} + I_{\text{ext}} + I_{\text{noise}}. \quad (1)$$

In the above equation, there are three kinds of current affecting the membrane potential dynamics: ionic current I_{ion} , external stimulus current I_{ext} , and noisy current I_{noise} . The membrane potential can change when two types of ions, the sodium(Na) ions and the potassium(K) ions, flow through the channels in the membrane, which produces the ionic current. All ionic movements across the membrane occur through

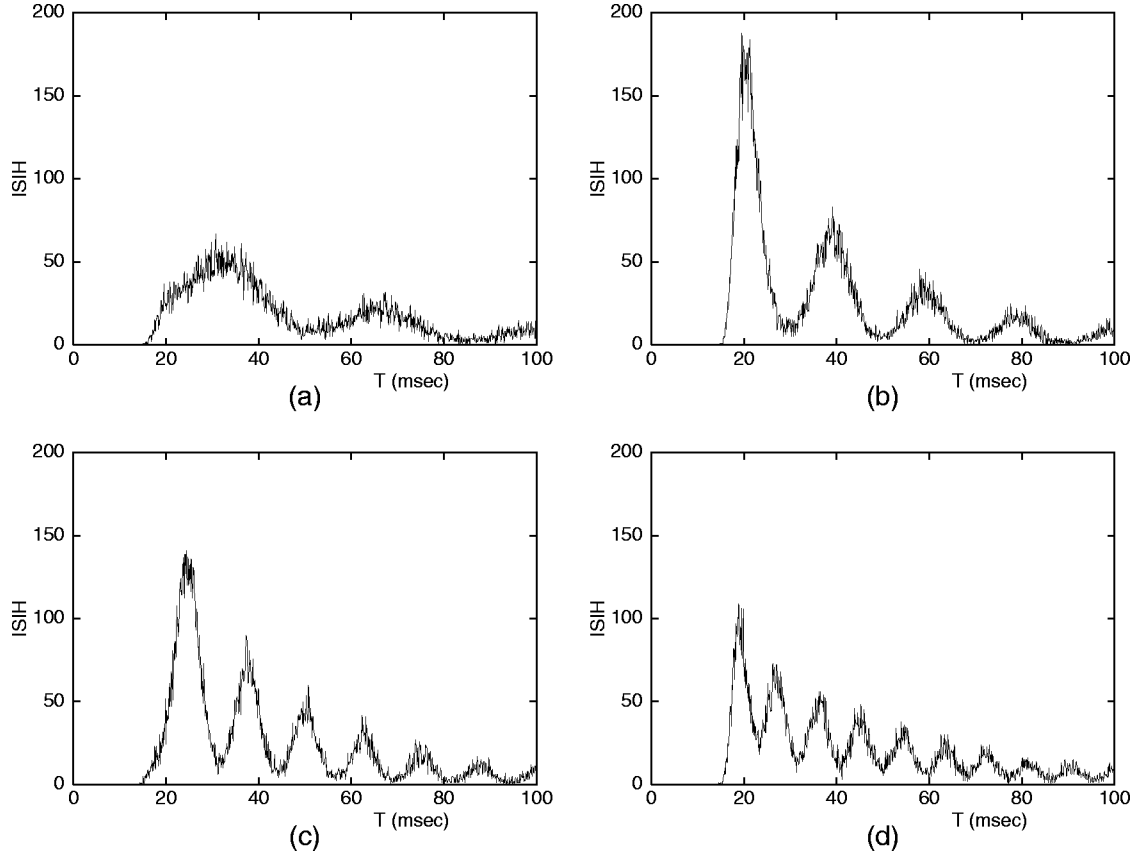


FIG. 1. Interspike interval histograms (ISIHs) of a stochastic Hodgkin-Huxley neuron under sinusoidal stimulus for different forcing frequencies (a) $f=30$ Hz, (b) $f=50$ Hz, (c) $f=80$ Hz, and (d) $f=110$ Hz. Here, $A_0=1 \mu\text{A}/\text{cm}^2$ and $D=5$.

channels permeable to a single ionic species and having two states; open or closed. The difference between the equilibrium potential of an ion and the membrane potential is the driving force for the ionic flow. The total conductance associated with any particular population of the ion channels can be expressed as the maximal conductance and the fraction of all channels that are open. The resultant ionic current from experiments by Hodgkin-Huxley [13] is written as,

$$I_{\text{ion}} = -g_{\text{Na}}m^3h(V - V_{\text{Na}}) - g_{\text{K}}n^4(V - V_{\text{K}}) - g_l(V - V_l), \quad (2)$$

where the constants g_{Na} , g_{K} , and g_l are maximal conductances for sodium, potassium, and leakage currents and V_{Na} , V_{K} , and V_l are corresponding reversal potentials,

$$\frac{dx}{dt} = \frac{x_\infty(V) - x}{\tau_x(V)}, \quad x = m, n, h. \quad (3)$$

The parameters x_∞ and τ_x in Eq. (1) represent the stationary values and the relaxation times for given membrane potential V , respectively. Details on these parameter values can be found in [13–15].

In this study we take the external stimulus to be time-dependent sinusoidal current $I_{\text{ext}}(t) = A_0 \cos(2\pi ft)$, where A_0 is set to be the *subthreshold* current amplitude and f the forcing frequency, and t the time in unit of milliseconds(ms). The noisy current $I_{\text{noise}} = I_0 \eta(t)$ represents the noisy compo-

nent of the stimulus in a neuron. Here, $I_0 = 1 \mu\text{A}/\text{cm}^2$ is a unit current and $\eta(t)$ is a zero mean Ornstein-Uhlenbeck(OU) process,

$$\tau_d \frac{d\eta}{dt} = -\eta + \xi(t), \quad (4)$$

where $\langle \xi(t) \rangle = 0$ and $\langle \xi(t)\xi(s) \rangle = 2D\delta(t-s)$. Here, D and τ_d are the noise intensity and the correlation time of the OU noise. In our numerical study, we take $\tau_d = 2$ ms. Numerical integration of the HH neuron in Eqs. (1) and (3) is carried out with a fourth order Runge-Kutta algorithm and that of the OU noise in Eq. (4) with the integral algorithm proposed by Fox *et al.* [16] with an integration time step of 0.02 ms.

Typically, neurons show resettable dynamics [3]. The neuron fires when it is excited above a threshold, and then is reset to the rest state after a refractory period. It has been well known that a major component of neural information in the nervous system is coded in the firing times of action potentials, or spikes [17]. If t_i denotes a sequence of spiking times with action potentials, the quantity $T_i = t_i - t_{i-1}$ represents the interspike interval between two subsequent spike events. To characterize the statistical properties of these spike intervals, an ensemble average of neuronal firing data is widely used in the form of the interspike interval histogram (ISIH), in which the time intervals between successive spikes are assembled into a single histogram. This ISIH of a stochastic neuron corresponds to the residence time distribu-

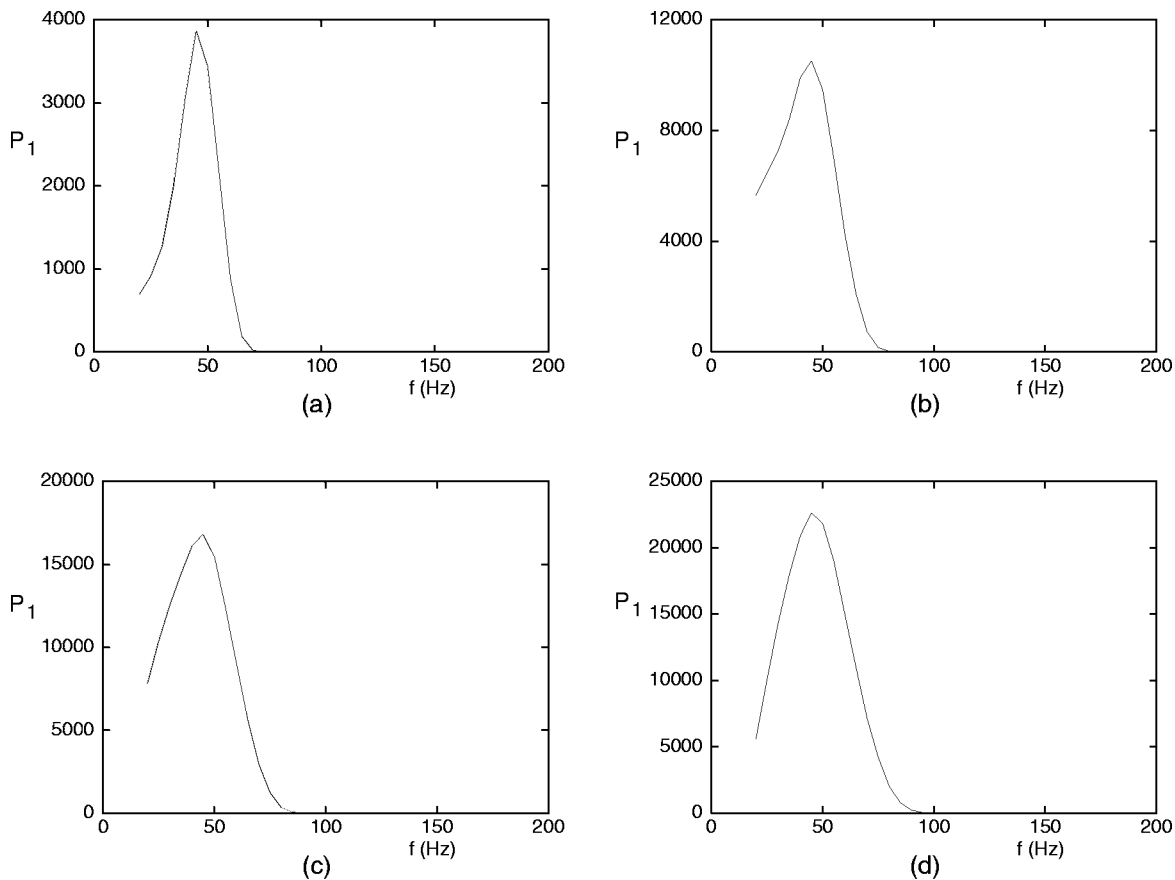


FIG. 2. Strength of P_1 peaks in the distribution of interspike intervals for different noise intensities of (a) $D=2$, (b) $D=5$, (c) $D=10$, and (d) $D=20$. Stimulus current is $A_0=1 \mu A/cm^2$.

tion in the bistable system. The ISIH for a stochastic Hodgkin-Huxley neuron shows a sequence of decaying peaks as in Fig. 1, and this exponential decay with peaks are similar to the residence time distribution in the bistable system. The maxima in the amplitudes of modes are located at integer multiples of the stimulus period, and decay, in general, for higher harmonics. Note that there are no peaks in ISIHs for $T_i < 20$ ms in Figs. 1(a)–1(d) due to the existence of the refractory period, which is different from the residence time distribution in the bistable system. The strength of the n th peak in the distribution function $N(T)$ in ISIH is defined by [8]

$$P_n = \int_{T_n - \alpha T_0}^{T_n + \alpha T_0} N(T) dT,$$

with $0 < \alpha \leq \frac{1}{4}$. The choice of the parameter α is found to be not relevant to our analysis. Here we use $\alpha = \frac{1}{4}$.

We have calculated the strength of P_1 and P_2 in the stochastic Hodgkin-Huxley neuron for various noise intensities and forcing frequencies as shown in Figs. 2 and 3. The resonant peaks in P_1 and P_2 show different behaviors as the function of the forcing frequency when the noise intensity increases. The resonant peak in P_1 is located near $f=45$ Hz and stays there even when the noise intensity increases as in Fig. 2.

In Fig. 4(a), we show an example of neural activities with

two subsequent spikes in $320 < t < 370$ ms and three subsequent spikes in $500 < t < 570$ ms that contribute to the P_1 peak (the interspike interval is roughly 20 ms). From the neural activities in Fig. 4(a), we can draw phase portraits as in Figs. 4(b) and 4(c). The orbits corresponding to fluctuations without spikes are found in the region A (near the rest state). On the other hand, the orbits corresponding to the spikes are the clockwise loop from the phase points near B with $dh/dt < -0.02$ to those near C with $dh/dt < 0.01$. The average time for this clockwise loop from B to C is $\langle T_{sp} \rangle \sim 15.93 \pm 0.54$ ms. The orbits that contribute to the P_1 peak correspond to one from B to the excitable point C without entering the region A. The time for this clockwise loop is called as the excitable time $\langle T_{exc} \rangle$. At the phase point C, the neuron can generate another action potential. Thus, the action potentials contribute the P_1 peak correspond to the clockwise loops from the phase point B back to B without entering the region A, which serve as quasistable oscillations. The time $\langle T_{exc} \rangle$ is roughly 4 ms, which is nearly constant for most noise intensities and forcing frequencies explored. Therefore, the resonance condition is $1/f \sim \langle T_{sp} \rangle + \langle T_{exc} \rangle$. The time $\langle T_{sp} \rangle + \langle T_{exc} \rangle$ for a loop is roughly 20 ms and it is the inverse of the natural frequency of the Hodgkin-Huxley neuron, that is, $f=50$ Hz [10]. The noise-induced transitions from the phase point in the region A (the rest state) to the point B (the quasistable oscillation) do not contribute to the P_1 peak at the resonant frequency. That is, this resonance is

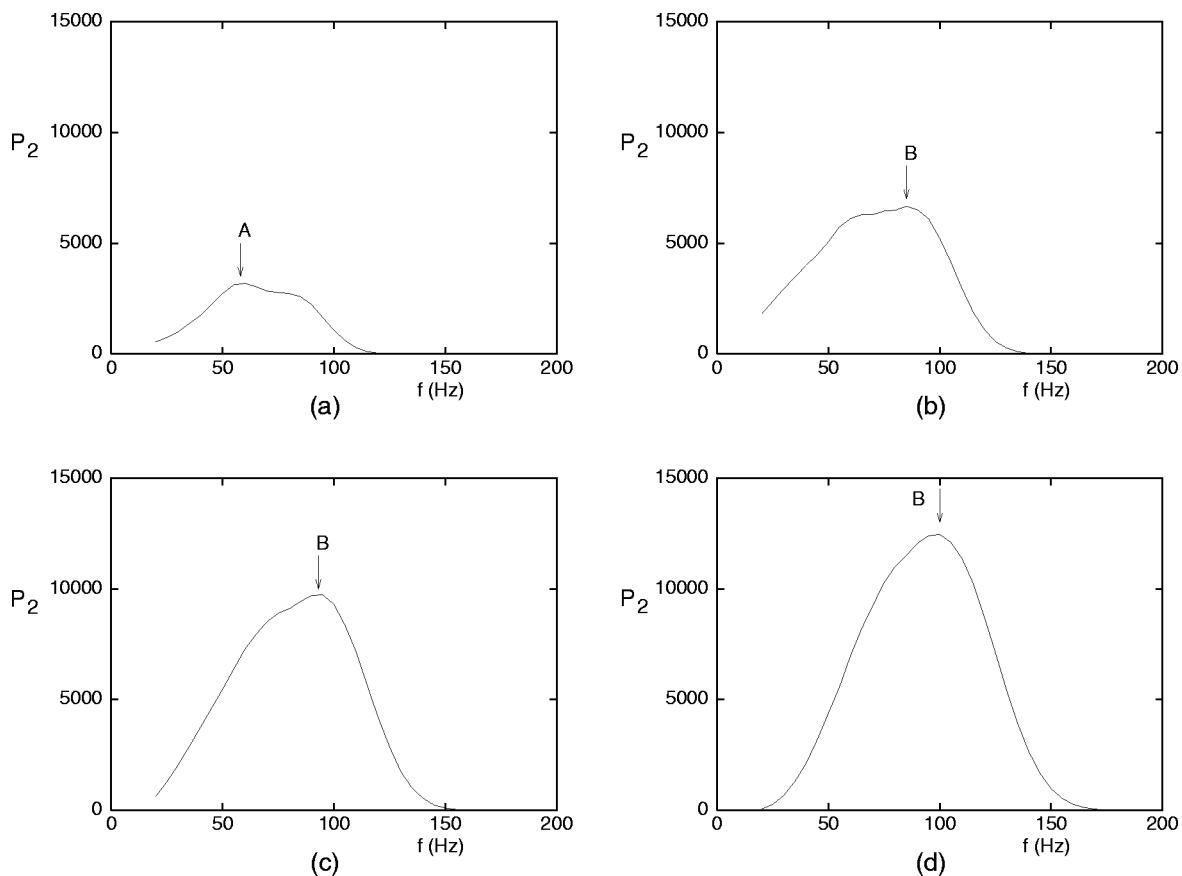


FIG. 3. Strength of P_2 peaks for different noise intensities of (a) $D=2$, (b) $D=5$, (c) $D=10$, and (d) $D=20$. Stimulus current is $A_0 = 1 \mu\text{A}/\text{cm}^2$.

not related to the stochastic time scale of noise-induced switching, so that the corresponding peak in P_1 does not move as the noise strength changes.

The resonant peaks in P_2 show somewhat different behavior, having a strong dependence on the noise intensity. There is a resonant peak A near $f=55$ Hz at small noise intensity as in Fig. 3(a). This peak is located at a slightly higher frequency than the natural frequency of the Hodgkin-Huxley neuron. At this resonant frequency, many interspike intervals are observed in the spike train, which has roughly twice the inverse of the natural frequency. These interspike intervals contribute to the P_2 peak, that is, this resonant peak A represents the second harmonic resonance between the natural frequency and forcing frequency. The resonant frequency for the peak labeled B increases as the forcing frequency is increased as in Figs. 3(b)–3(d). This dependence of the resonant frequency on the noise intensity suggests that the stochastic time scale contributes to this resonance.

In order to understand the detailed mechanisms behind this resonance, the neural activities at the forcing frequency $f=80$ Hz are shown in Fig. 5(a) and their corresponding phase portrait in Fig. 5(b). We find subsequent action potentials contributing to P_2 peaks in $100 < t < 150$ ms and $400 < t < 450$ ms in Fig. 5(a). The average time for the spike $\langle T_{\text{sp}} \rangle$ in the phase portrait from B to C through a clockwise loop is $\langle T_{\text{sp}} \rangle \sim 15.90 \pm 1.49$ ms, which is similar to that for the forcing frequency $f=50$ Hz. In this case, the trajectories

enter the region A after an action potential and, after a while, this phase point moves out to the spike initiation point B , which is the noise-induced transition from the rest state in A to the spike initiation point B . The condition for a inter-spike interval contributing to the P_2 peak is $2T - (T/2) < T_{\text{sp}} + T_k < 2T + (T/2)$, where T_k is the average escape time for the phase points to move out of the region A . This suggests a resonance condition, $2T = \langle T_{\text{sp}} \rangle + \langle T_k \rangle$. We have measured $\langle T_k \rangle$ as a function of the noise intensity, which shows a sharp decay as in Fig. 6. Thus, when we increase the noise intensity, the resonant frequency also increases because the noise-induced escape time $\langle T_k \rangle$ becomes smaller.

The phase relation between the periodic forcing and the response of the stochastic system is an important issue in the stochastic resonance [18]. In our study, we have focused our attention on the shape of the distribution of the phases. For this purpose, an order parameter is introduced to quantify the phase relationship between the sinusoidal input current and the neural responses. Define the phase θ_k for the k th spike as the phase of the sinusoidal current at the spike. If the spikes are well synchronized to the sinusoidal input current, the phases are similar to each other. In this case, the angular distribution of θ_k shows a localized structure. On the other hand, if the spikes are not well synchronized, the distribution shows a broadly distributed structure. The distribution of the phases can be represented by a complex quantity,

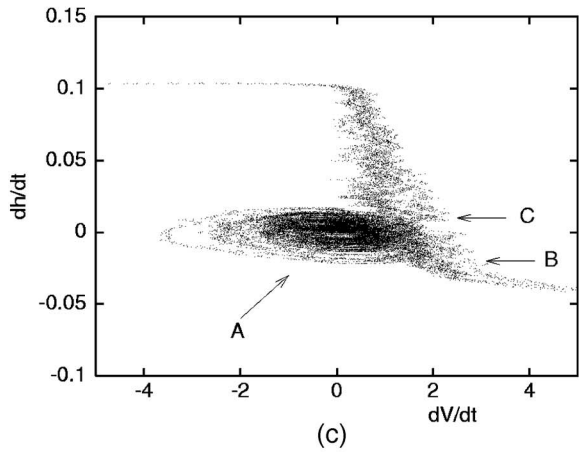
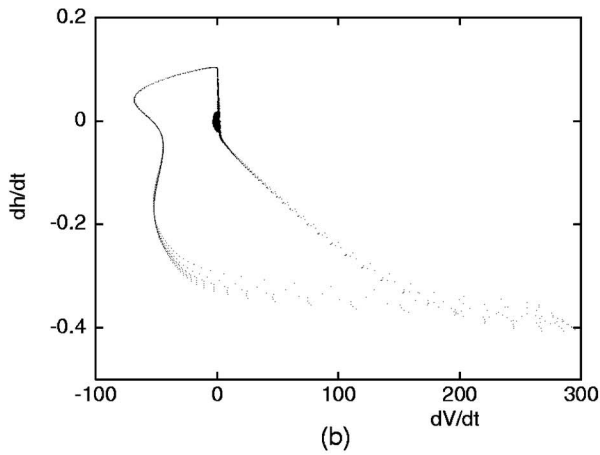
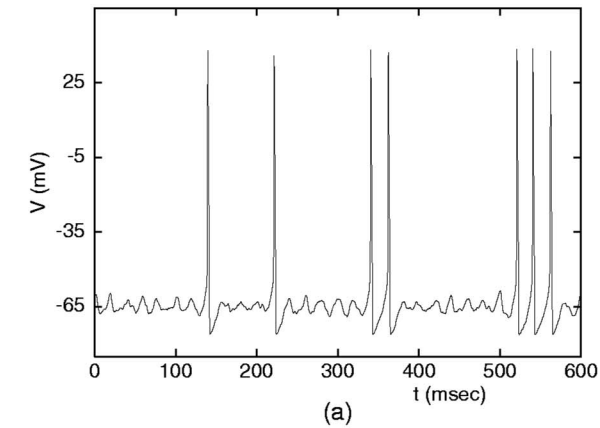


FIG. 4. (a) The membrane potential at the noise intensity $D=1$ and forcing frequency $f=50$ Hz. (b) The phase portrait in the phase space of $(dV/dt, dh/dt)$ for the spike train in (a). (c) The magnification of (b) near $(0,0)$. Noise induced fluctuations are found near the region A, where B and C indicate the spike initiation point ($dh/dt=-0.02$) and end point ($dh/dt=0.01$), respectively.

$$\sigma e^{i\Theta} = \sum_k^{N_a} e^{i\theta_k}$$

Here N_a is the number of action potentials for a given time interval. The magnitude σ of the complex quantity can serve

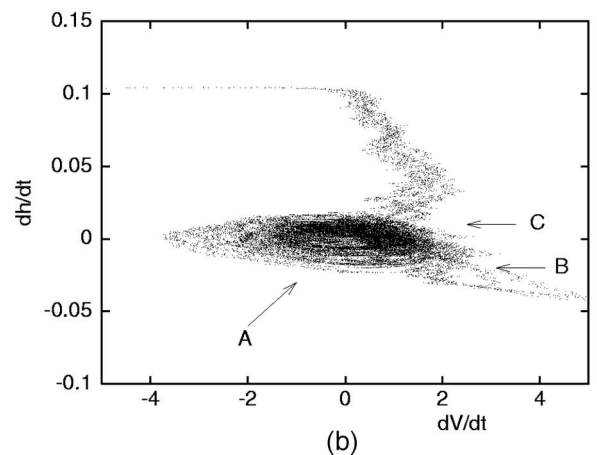
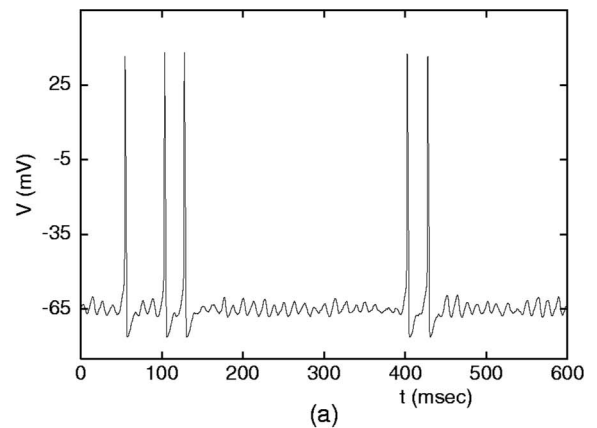


FIG. 5. (a) The membrane potential at the noise intensity $D=1$ and forcing frequency $f=80$ Hz. (b) The phase portrait $(dV/dt, dh/dt)$ for the spike train in (a). Noise induced fluctuation is in region A, and arrows B, C indicate the action potential initiation point ($dh/dt=-0.02$) and end point ($dh/dt=0.01$), respectively.

as an order parameter which characterizes the degree of phase synchronization between the periodic forcing and the action potentials. Clearly, σ vanishes for the uniform distribution without phase synchronization, whereas it shows

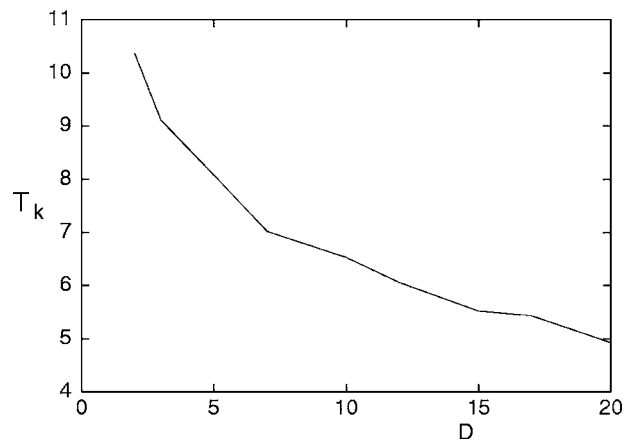


FIG. 6. The averaged time $\langle T_k \rangle$ as the function of D .

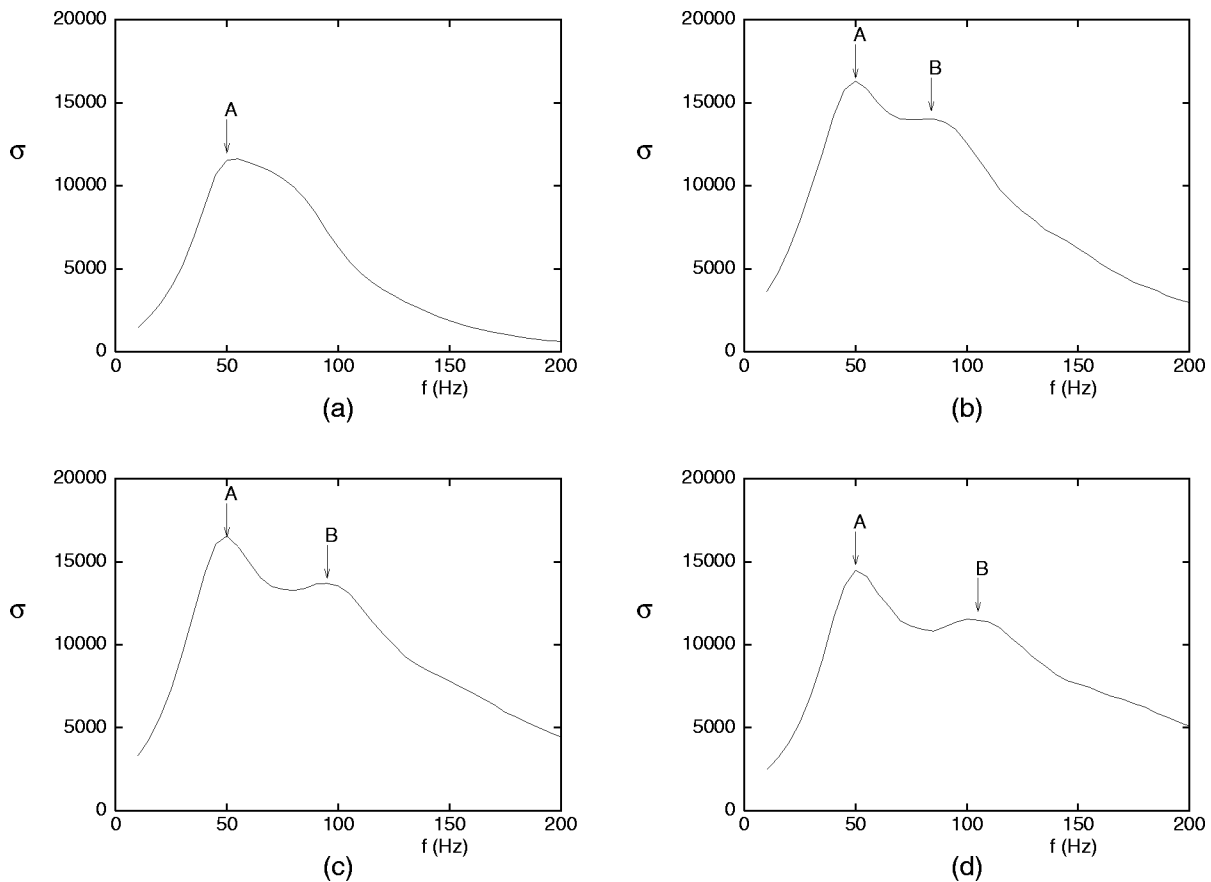


FIG. 7. Order parameter σ for phase synchronization for different noise intensities of (a) $D=2$, (b) $D=5$, (c) $D=10$, and (d) $D=20$. Stimulus current is $A_0=1 \mu\text{A}/\text{cm}^2$.

sharp peak when there is a strong phase synchronization.

The order parameter have been computed as the function of the forcing frequency as in Fig. 7(a), which shows one peak at small noise intensity in Fig. 7(a), and two peaks at strong noise intensity in Figs. 7(b)–7(d). The first peak A is located near $f \sim 45$ Hz and does not change even under the strong noise influence. This resonant frequency corresponds to that in the P_1 distribution. On the other hand, the resonant frequency for the second peak B increases as the noise intensity increases, the location of which corresponds to that in the P_2 distribution (compare Fig. 3 with Fig. 7). The resonant peaks observed in ISIH correspond to the peaks in the order parameter analysis. This observation suggests that the bona fide stochastic resonance in the stochastic Hodgkin-Huxley neuron is originated from the phase synchronized firings to the periodic forcing.

As recently observed in [19], the background noise underlying the peaks can lead to an erroneous evaluation of the strength of the peaks in the ISIH distribution function. In fact, the intensity of the background in the distribution shows a resonant behavior even when there is no periodic modulation. The resonance structure in the modified ISIH \tilde{N} after the subtraction of the background ISIH must be studied to find out the true resonance by the periodic forcing. We first calculate the ISIH curve for a small forcing amplitude of $A_0=0.2 \mu\text{A}/\text{cm}^2$. In this case of weak periodic stimulus, the background does not depend appreciably on the modulation

amplitude [4,20]. The subtraction between two ISIH curves for $A_0=0 \mu\text{A}/\text{cm}^2$ and $A_0=0.2 \mu\text{A}/\text{cm}^2$ represents synchronous switches corresponding to the periodic forcing. We find that \tilde{P}_1 shows a resonant peak nearly at the same frequency of $f=45$ Hz as one for P_1 and the same is true for \tilde{P}_2 and P_2 . We get similar results for \tilde{N} with $A_0=0 \mu\text{A}/\text{cm}^2$ and $1 \mu\text{A}/\text{cm}^2$.

For the purpose of the comparison, the background decay function is calculated from the fitting curves as in [20,21]. The ISIH in the excitable system has an exponential decay for a relatively large time interval of roughly $T > 20$ ms and vanishes in the time interval of $T < 15$ ms because the neuron cannot fire during the refractory period (see Fig. 1). Here the exponential decay function is calculated by fitting the minima in the ISIH curve when $T > 20$ ms. \tilde{N} is calculated by subtracting the background exponential decay from the ISIH curve. Note that \tilde{N} is set to zero when the decay function is larger than ISIH for small intervals (roughly $T < 20$ ms). \tilde{P}_1 obtained from this curve of \tilde{N} shows a resonant peak at $f=45$ Hz and \tilde{P}_2 shows a resonant structure similar to one from P_2 . We find from this comparison study between resonant structures in N and \tilde{N} that the resonance in N is caused by the nonlinear interaction between three frequencies and not by the background noise.

For comparison with the results of the HH neuron, we also studied the bona fide SR in the stochastic FitzHugh-

Nagumo neuron. The stochastic FitzHugh-Nagumo neuron model is given by [22–24],

$$\begin{aligned} \epsilon \frac{dv}{dt} &= v(v-a)(1-v) - w + \xi(t), \\ \frac{dw}{dt} &= v - dw - b - A_0 \cos(2\pi ft), \end{aligned} \quad (5)$$

where $\langle \xi(t) \rangle = 0$ and $\langle \xi(t)\xi(s) \rangle = 2D\delta(t-s)$. Here, $\epsilon=0.005$ and $a=0.5$, $d=1.0$, and $b=0.12$. In this model, we have focused our attention on the structure of the P_1 peak and its dependence on the noise intensity as in Fig. 8(a). Interestingly, the P_1 peak increases as the noise intensity increases, which is different from the case of the P_1 peak in the stochastic HH neuron in Fig. 2, but rather similar to the case of the P_2 peak in Fig. 3. To understand this difference in behaviors of P_1 peaks, we studied the phase portraits of the stochastic FitzHugh-Nagumo neuron in Fig. 8(b). The action potential corresponds to a counter-clockwise curve starting from near $(v, w) = (0.4, -0.04)$ to $(0, 0)$ in Fig. 8(b). The orbit enters the stable state region near $(0.2, -0.04)$ after a generation of the action potential and, after a while, it move out to the spike initiation point, which is the noise-induced transition from the rest state to an action potential. So the resonant frequency also increases as the noise intensity increases because the noise-induced escape time becomes smaller. Even though both the stochastic HH neuron and the stochastic FitzHugh-Nagumo neuron have three relevant time scales, they show different bona-fide SR structures.

In this study, we have observed the bona fide SR in the stochastic Hodgkin-Huxley neuron as the periodic forcing frequency is varied. Due to the existence of the inherent natural frequency in the stochastic Hodgkin-Huxley neuron, we find two different types of resonances as the forcing frequency is varied. Deterministic resonance occurs between the forcing frequency and the natural frequency near $f = 50$ Hz and stochastic resonance occurs between forcing frequency and the stochastic time scale. This multimodal resonance is different from the one in the bistable system with only one peak. An order parameter is introduced in this paper to measure the averaged phase synchronization between the periodic forcing and the spikes. This order parameter also shows the resonant peaks nearly at the same frequencies observed in strengths of ISIH. This similarity in the resonant frequencies shows that the bona fide stochastic resonance in the stochastic Hodgkin-Huxley neuron is originated from the

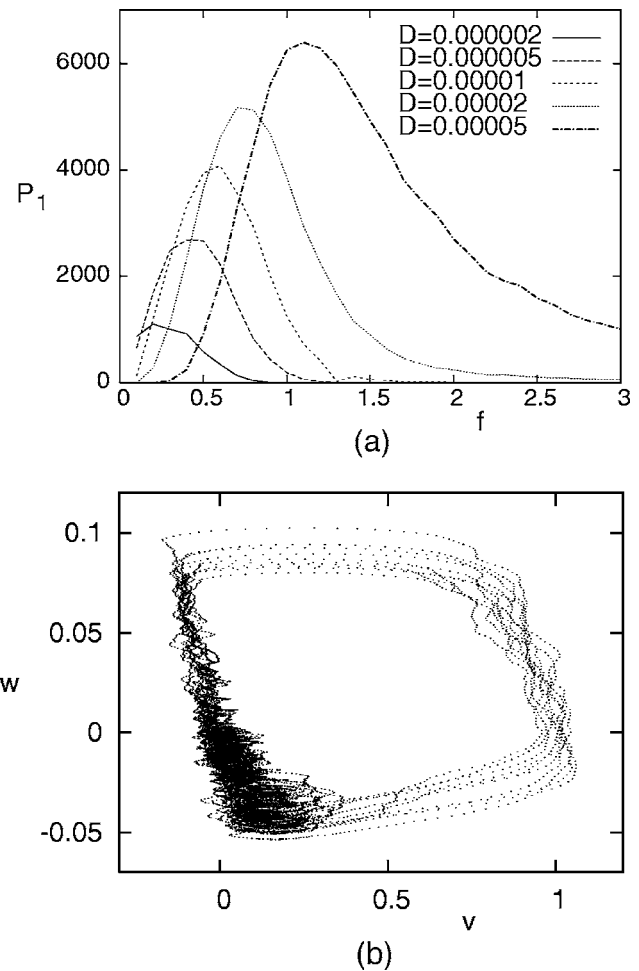


FIG. 8. (a) The strength of P_1 peaks in the distribution of interspike intervals for different noise intensities in the stochastic FitzHugh-Nagumo neuron with $A_0=0.1$. (b) The phase portraits in the phase space of (v, w) for the spike train at the noise intensity $D=0.000005$ and the forcing frequency $f=0.5$.

phase synchronization. Our understanding of resonance phenomena in the stochastic Hodgkin-Huxley neuron may provide a useful tip for the understanding of the bona fide SR in many excitable systems.

This work was supported by the National Core Research Center on System BioDynamics and by the Brain Research Project of the Ministry of Science and Technology and by the Ministry of Education in Korea.

[1] R. Benzi, A. Sutera, and A. Vulpiani, *J. Phys. A* **14**, L453 (1981); R. Benzi, G. Parisi, A. Sutera, and A. Vulpiani, *Tellus* **34**, 10 (1982); C. Nicolis, *ibid.* **34**, 1 (1982).
 [2] F. Moss, A. Bulsara, and M. F. Shlesinger, in *Proceedings of the NATO Advanced Research Workshop on Stochastic Resonance in Physics and Biology*, *J. Stat. Phys.* **70**, 1 (1993); R. Mannella and P. V. E. McClintock, in *Proceedings of the In-*

ternational Workshop on Fluctuations in Physics and Biology: Stochastic Resonance, Signal Processing and Related Phenomena, *Nuovo Cimento D* **17**, 661 (1995).
 [3] F. Moss, D. Pierson, and D. O’Gorman, *Int. J. Bifurcation Chaos Appl. Sci. Eng.* **4**, 1383 (1994); K. Wiesenfeld and F. Moss, *Nature (London)* **373**, 33 (1995); A. R. Bulsara and L. Gammitoni, *Phys. Today* **49**, 39 (1996).

- [4] L. Gammitoni, P. Hänggi, P. Jung, and F. Marchesoni, *Rev. Mod. Phys.* **70**, 223 (1998).
- [5] K. Wiesenfeld, D. Pierson, E. Pantazelou, C. Dames, and F. Moss, *Phys. Rev. Lett.* **72**, 2125 (1994).
- [6] A. Longtin, *J. Stat. Phys.* **70**, 309 (1993).
- [7] F. Moss, *Ber. Bunsenges. Phys. Chem.* **95**, 303 (1991).
- [8] L. Gammitoni, F. Marchesoni, and S. Santucci, *Phys. Rev. Lett.* **74**, 1052 (1995).
- [9] A. Longtin and D. R. Chialvo, *Phys. Rev. Lett.* **81**, 4012 (1998); B. Lindner and L. Schimansky-Geier, *Phys. Rev. E* **61**, 6103 (2000); D. T. W. Chik, Y. Wang, and Z. D. Wang, *ibid.* **64**, 021913 (2001); G. Schmid, I. Goychuk, and P. Hänggi, *Europhys. Lett.* **56**, 22 (2001); T. Prager and L. Schimansky-Geier, *Phys. Rev. Lett.* **91**, 230601 (2003).
- [10] S. G. Lee, Ph. D. thesis, Pohang University of Science and Technology (POSTECH), 1999; S. G. Lee and S. Kim (unpublished).
- [11] A. S. Pikovsky and J. Kurths, *Phys. Rev. Lett.* **78**, 775 (1997).
- [12] S. G. Lee, A. Neiman, and S. Kim, *Phys. Rev. E* **57**, 3292 (1998).
- [13] A. L. Hodgkin and A. F. Huxley, *J. Physiol. (London)* **117**, 500 (1952).
- [14] S. G. Lee, S. Kim, and H. Kook, *Int. J. Bifurcation Chaos Appl. Sci. Eng.* **7**, 889 (1997).
- [15] D. Hansel, G. Mato, and C. Meunier, *Europhys. Lett.* **23**, 367 (1993).
- [16] R. F. Fox, I. R. Gatland, R. Roy, and G. Vemuri, *Phys. Rev. A* **38**, 5938 (1988).
- [17] E. R. Kandel, J. H. Schwartz, and T. J. Jessell, *Principles of Neural Science* (Elsevier, New York, 1991).
- [18] M. I. Dykman, R. Mannella, P. V. E. McClintock, and N. G. Stocks, *Phys. Rev. Lett.* **68**, 2985 (1992).
- [19] M. H. Choi, R. F. Fox, and P. Jung, *Phys. Rev. E* **57**, 6335 (1998).
- [20] F. Marchesoni, L. Gammitoni, F. Apostolico, and S. Santucci, *Phys. Rev. E* **62**, 146 (2000).
- [21] G. Giacomelli, F. Marin, and I. Rabbiosi, *Phys. Rev. Lett.* **82**, 675 (1999).
- [22] J. C. Alexander, E. J. Doedel, and H. G. Othmer, *SIAM J. Appl. Math.* **50**, 1373 (1990).
- [23] A. Longtin, *Chaos* **5**, 209 (1995).
- [24] A. Longtin, *IL Nuovo Cimento* **17**, 835 (1995).